European Journal of Cell Biology 96 (2017) 61–69

Contents lists available at ScienceDirect

European Journal of Cell Biology

journal homepage: www.elsevier.com/locate/ejcb

Research paper

Dynamical modeling of liver Aquaporin-9 expression and glycerol permeability in hepatic glucose metabolism

Patrizia Gena[a], Nicoletta Del Buono[b], Marcello D'Abbicco[b], Maria Mastrodonato[c], Marco Berardi[d], Maria Svelto[a], Luciano Lopez[b], Giuseppe Calamita[a,*]

[a] Dipartimento di Bioscienze, Biotecnologie e Biofarmaceutica, Università degli Studi di Bari "Aldo Moro", via Orabona, 4-70125 Bari, Italy
[b] Dipartimento di Matematica, Università degli Studi di Bari "Aldo Moro", via Orabona, 4-70125 Bari, Italy
[c] Dipartimento di Biologia, Università degli Studi di Bari "Aldo Moro", via Orabona, 4-70125 Bari, Italy
[d] Istituto di Ricerca sulle Acque, Consiglio Nazionale delle Ricerche (CNR), via De Blasio, 5-70132 Bari, Italy

ARTICLE INFO

Article history:
Received 26 August 2016
Received in revised form
18 December 2016
Accepted 19 December 2016

Keywords:
Glucose homeostasis
Insulin
Membrane glycerol permeability
Aquaglyceroporin channels
Differential equations
Least-squared approximation

ABSTRACT

Liver is crucial in the homeostasis of glycerol, an important metabolic intermediate. Plasma glycerol is imported by hepatocytes mainly through Aquaporin-9 (AQP9), an aquaglyceroporin channel negatively regulated by insulin in rodents. AQP9 is of critical importance in glycerol metabolism since hepatic glycerol utilization is rate-limited at the hepatocyte membrane permeation step. Glycerol kinase catalyzes the initial step for the conversion of the imported glycerol into glycerol-3-phosphate, a major substrate for *de novo* synthesis of glucose (gluconeogenesis) and/or triacyglycerols (lipogenesis). A model addressing the glucose-insulin system to describe the hepatic glycerol import and metabolism and the correlation with the glucose homeostasis is lacking so far. Here we consider a system of first-order ordinary differential equations delineating the relevance of hepatocyte AQP9 in liver glycerol permeability. Assuming the hepatic glycerol permeability as depending on the protein levels of AQP9, a mathematical function is designed describing the time course of the involvement of AQP9 in mouse hepatic glycerol metabolism in different nutritional states. The resulting theoretical relationship is derived fitting experimental data obtained with murine models at the fed, fasted or re-fed condition. While providing useful insights into the dynamics of liver AQP9 involvement in male rodent glycerol homeostasis our model may be adapted to the human liver serving as an important module of a whole body-model of the glucose metabolism both in health and metabolic diseases.

1. Introduction

Aquaporin-9 (AQP9) is a protein belonging to *Aquaglyceroporins*, a branch of the Aquaporin family of channels facilitating transport of glycerol and water across biological membranes (Agre, 2004; Gena et al., 2011; Hara-Chikuma and Verkman, 2006). AQP9 features broad selectivity allowing transport of a wide variety of non-charged solutes including urea, carbamides, nucleosides, monocarboxylates, purines, pyrimidines and metalloid arsenic besides to glycerol and other polyols (Liu et al., 2002; Tsukaguchi et al., 1998). In rodents, AQP9 is mainly expressed in liver parenchyma, at the sinusoidal plasma membrane of hepatocytes (Elkjaer et al., 2000). At lower extent rodent AQP9 is also found in other body districts including peripheral leucocytes, epididymis, *vas deferens*, epidermis and brain (Badaut et al., 2004; Ishibashi et al., 1998; Pastor-Soler et al., 2001; Rojek et al., 2007). AQP9 expression in human tissues appears to be more selective than in mice (Lindskog et al., 2016). In rodents, AQP9 is the major pathway through which glycerol is imported from portal blood to hepatocytes during short-term fasting (Calamita et al., 2012; Jelen et al., 2011). As soon as it is imported, glycerol is readily converted by glycerol kinase into glycerol-3-phosphate (G3P), an important substrate for *de novo* synthesis of glucose (gluconeogenesis) making glycerol of pivotal importance in nutritional states requiring high glucose production (Bernardino et al., 2016; Brisson et al., 2001; Calamita et al., 2012; Calamita et al., 2015; Jelen et al., 2011). Hepatocyte AQP9 is also involved in lipid homeostasis being G3P a key substrate also for triacylglycerols (TAGs) synthesis (Rodriguez et al.,

Abbreviations: AQP9, Aquaporin-9; G3P, glycerol-3-phosphate; glycoAQP9, N-glycosylated AQP9; ODE, ordinary differential equation; TAG, triacylglycerol; S.E.M., standard error of the mean.

* Corresponding author at: Dipartimento di Bioscienze, Biotecnologie e Biofarmaceutica, Università degli Studi di Bari "*Aldo Moro*", Via E. Orabona, 4-70125 Bari, Italy.
E-mail address: giuseppe.calamita@uniba.it (G. Calamita).

http://dx.doi.org/10.1016/j.ejcb.2016.12.003
0171-9335/

2011a; Lebeck, 2014). AQP9 has also been reported to contribute to rodent bile formation (Calamita et al., 2008) and catabolic urea extrusion (Jelen et al., 2012). In rodents, hepatocyte AQP9 is negatively regulated by insulin at the transcriptional level (Kuriyama et al., 2002) explaining why states of insulin resistance are accompanied by increased AQP9 (Calamita et al., 2015; Carbrey et al., 2003). Indicating relevance of AQP9 in glucose and lipid metabolism and energy balance, mice lacking AQP9 have reduced liver glycerol permeability associated with increased levels of plasma glycerol and TAGs (Calamita et al., 2012; Rojek et al., 2007). Mouse models of obesity (specifically *ob/ob* mice) show reduced levels of hepatocyte AQP9 accompanied with a significant decrease of the liver glycerol permeability (Gena et al., 2013). A similar situation is seen in obese patients with type 2 diabetes (Rodriguez et al., 2014). These observations have been interpreted as a compensatory mechanism aimed at contrasting both the ectopic accumulation of TAGs into hepatocytes and the progression of hyperglycemia (Gena et al., 2013; Rodriguez et al., 2014; Rodriguez et al., 2015b). Hepatocyte AQP9 is also modulated by leptin (Rodriguez et al., 2011b, 2015b) although the regulation exerted by both insulin and leptin on the expression of the *Aqp9* gene appears to be different when comparing rodents with humans (for reviews see Calamita et al., 2015 and Lebeck, 2014). The expression of AQP9 is regulated at multiple levels as liver AQP9 undergoes sex-specific dimorphism both in humans and rodents (for review see Rodriguez et al., 2015a). This may reflect a more general situation regarding the handling of glycerol in the two sexes because gender-dependent differences have been also observed regarding two other metabolically important aquaglyceroporins, AQP3 and AQP7, in the adipose tissue (for review see Rodriguez et al., 2015a).

Although a series of kinetic mathematical models of hepatic glucose metabolism are already available (Bulik et al., 2016) a model integrating the hepatic import and handling of glycerol in the glucose-insulin system is lacking, so far. Recently, we started to approach the question by describing a model for the hepatic glucose metabolism based on Hill and step functions (D'Abbicco et al., 2016) as initial step in modeling the (*i*) refilling/depletion of glycogen stores during the fed/fasted state, (*ii*) the influence of plasma glycerol and (*iii*) the liver glycerol permeability to the protein levels of hepatic AQP9 in glucose homeostasis. Here, we now report a system of nonlinear first-order ordinary differential equations to set up a mathematical model of the hepatic glucose metabolism taking into account AQP9 and its role in facilitating the entry of lipolytic glycerol into hepatocytes of male lean mice. A dataset of the time course of plasma glucose and circulating insulin integrated with the hepatic glycogen content is employed to simulate the expression of AQP9 and glycerol membrane permeability of mice in three different conditions of hepatic glucose metabolism, the fed, fasted and re-fed states. The obtained theoretical result agrees with the experimental data and represents a first attempt to mathematically describe changes of hepatic glycerol permeability as a direct function of hepatocyte AQP9 protein.

2. Materials and methods

2.1. Animals

Seven-week-old male C57BL/6J mice (Envigo RMS srl, S. Pietro al Natisone, Italy) were allowed free access to a standard laboratory rodent diet (Altromin-Rieper, Vandoies, Italy) and water *ad libitum*. For the experiments of fasting and re-feeding, the fasted group (four to six animals for each time point) was starved for 2, 4, 8, 10, 14, 18, 20, 24, 30, 36, 42 or 48 h before being sacrificed by cervical dislocation while the fasted/re-fed group of animals had free access to diet for 12, 24, 36, 48, 60 or 72 h after 48 h of fasting. Animals were housed in air-conditioned room with 12/12 h dark-light cycle. All the studies have been approved by the animal care and use Committee of the University of Bari (OPBA di Ateneo) and the Italian Ministry of Health.

2.2. Analytical procedures

Plasma glucose levels were measured using an Accu-Check Sensor (Roche Diagnostics, Mannheim, Germany) and a drop of tail vein blood. For plasma glycerol analysis, blood samples were collected from the right cardiac ventricle into heparinized tubes and centrifuged for 10 min at 4,000x*g* to remove blood cells. Plasma glycerol concentrations were determined by using a colorimetric enzyme method following the manufacturer's instructions (EnzyChrom™ Glycerol Assay Kit, BioAssay System, Hayward, CA). Plasma insulin was assayed by an ELISA kit as recommended by the manufacturer (Millipore, Billerica, MA).

2.3. Preparation of hepatocyte sinusoidal plasma membrane vesicles

The sinusoidal plasma membrane fraction of mouse hepatocytes was prepared as previously described (Calamita et al., 2012). Briefly, livers were quickly removed after the sacrifice and homogenized with a Potter-Elvehjem homogenizer (15 strokes at 500 rpm) in an ice-cold isolation medium consisting of 220 mM mannitol, 70 mM sucrose, 20 mM Tris-HCl, 1 mM EDTA and 5 mM EGTA, pH 7.4, added of a cocktail of protease inhibitors (1 mM PMSF, 1 mM leupeptin, 1 mM pepstatin A). The cell homogenate was centrifuged at 500X*g* for 10 min and the pellet consisting of nuclei and unbroken cells was discarded; the resulting supernatant was centrifuged at 8,000X*g* for 20 min. The related pellet containing mainly mitochondria was discarded, whereas the supernatant was centrifuged at 12,000 × *g* for 15 min. The resulting pellet enriched in the sinusoidal fraction of hepatocyte sinusoidal plasma membrane was collected and the protein concentration assayed by the Lowry method. All centrifugations were carried out at 4 °C. Enrichment and purity of isolated sinusoidal membranes were comparable to those previously reported (Marinelli et al., 2003). All chemicals were purchased from Sigma Chemical Company (St. Louis, MO).

2.4. Immunoblotting analysis

Aliquots (30 μg of proteins) of hepatocyte sinusoidal membranes prepared as above were heated to 90 °C for 5 min and electrophoresed in an SDS 13% acrylamide gel (Mighty Small II, Amersham Biosciences, CA) using a low molecular weight protein ladder (GE Healthcare, Buckinghamshire, UK). The resolved proteins were submitted to immunoblotting using anti-ratAQP9 antibodies (1 μg/ml; Alpha Diagnostics International, San Antonio, TX) as previously reported (Calamita et al., 2008). The immunoreactive bands were quantified by densitometry using ImageJ software (NIH, Bethesda, MD). The density of each band was normalized against that of the housekeeper protein β-actin.

2.5. Stopped-flow light scattering measurement of glycerol permeability

The size of the sinusoidal membrane-enriched vesicles prepared as described above was determined using a N5 Submicron Particle Size Analyzer (Beckman Coulter, Palo Alto, CA) and by transmission electron microscopy. The time course of vesicle volume change was followed from changes in scattered light intensity at 10 °C at the wavelength of 530 nm by using a BioLogic MPS-200 stopped flow reaction analyzer (BioLogic, Claix, France) that has a 1.6 ms dead time and 99% mixing efficiency in <1 ms. Light scattering

experiments were performed as previously described by submitting the vesicles to a 150 mM inwardly directed gradient of glycerol (Calamita et al., 2008; Calamita et al., 2012). Glycerol permeability coefficient (P_{gly}; cm/s) was computed by using the equation:

$$P_{gly} = 1/[(S/V)\tau]$$

where S/V is surface-to-volume ratio and τ is the exponential time constant fitted to the vesicle swelling phase of light scattering time course corresponding to glycerol entry.

2.6. Biochemical analysis of hepatic glycogen content

Glycogen was extracted from the liver of fed, fasted and fasted/re-fed mice by alkaline extraction (Sprangers et al., 1998), as previously described (Ferri et al., 2003). Briefly, extracted glycogen was hydrolyzed by treatment with amyloglucosidase at pH 4.7, and the related glucose was measured spectrophotometrically with adenosine triphosphate, oxidized nicotinamide adenine dinucleotide phosphate, glucose-6-phosphate dehydrogenase, and hexokinase.

2.7. Histochemistry

Samples of each mouse liver specimen were fixed in a 4% paraformaldehyde solution in 0.1 M phosphate-buffered saline (PBS) pH 7.4 at 4 °C for 3 h. Samples were then dehydrated with increasing acetone and embedded in Technovit 8100 kit (EMS, Hatfield, PA). Two microns thick sections were sequentially stained with Toluidine blue (TB)-periodic acid-Schiff (PAS). Digital pictures (original magnification: 400x) were taken for each sample using a Nikon Eclipse 600 photomicroscope equipped with a Nikon DMX 1200 camera (Nikon Instruments SpA, Calenzano, Italy).

2.8. Mathematical model

To describe the regulatory mechanism of the hepatic AQP9 protein output, later denoted by A, we employed a first-order ordinary differential equation (ODE) containing an insulin negatively regulated source term and a linear degradation rate, which is typical of proteins. To determine the linear degradation rate, based on our previous time-course expression study (Calamita et al., 2012), we assumed the hepatic AQP9 protein half-life approximately in 8 h. Since the degradation rate α satisfies $e^{-\alpha T} = 0.5$, where T = 8 h, we derive $\alpha = T^{-1}\log_e 2$, approximately, α = 0.038/hour. The value assigned to α did not influence the derivation of the devised model. The resulting equation describing the protein level of AQP9 was the following one:

$$dA/dt = h(I) - \alpha A$$

where h(I) is a function depending on the circulating plasma insulin I. If the insulin level is kept constant at the value I for a sufficiently large time, then A tends to the equilibrium point $A^{\dagger} = h(I)/\alpha$.

To mimic this, we decided to model the function h(I)/α so that it approximated the values obtained experimentally for I and A, at different time points, during the fasting state. The ODE regulating the expression of AQP9 and, consequently, the liver glycerol permeability, denoted by $P_{gly}(A)$, was then employed in the following abstract differential system:

$$dG/dt = f_1(G, I, \Gamma, P_{gly}(A))$$

$$dI/dt = f_2(G, I)$$

$$d\Gamma/dt = f_3(G, \Gamma)$$

$$dA/dt = h(I) - \alpha A$$

where the four variables are the hepatic glucose, G, the circulating plasma insulin I, the level of the glycogen stores Γ, and the AQP9 protein level, A.

The interplay between hepatic glucose, G, and glycogen stores, Γ, is regulated by the opposite processes of glycogenolysis and glycogen synthesis, in which glycogen is employed to produce glucose or vice versa. As far as the glycogen stores deplete, the glycogenolysis becomes less and less relevant. In prolonged fasting, the gluconeogenesis becomes more and more relevant for the hepatic glucose homeostasis as glycogen stores deplete. Several models for the glucose-insulin system have been proposed (Bulik et al., 2016; Chalhoub et al., 2007; Silber et al., 2010; Chen et al., 2010; Palumbo et al., 2013) some of them specifically addressing the glucose-insulin-glycogen system (König et al., 2012). A model for the hepatic glucose metabolism based on Hill and step functions (general expression of Hill function are presented and discussed is the *Results* section), has been recently developed by our group (D'Abbicco et al., 2016) starting from previous mathematical considerations indicating the importance of these functions in modeling biological dynamical systems (Del Buono et al., 2014).

The novelty in the proposed system is that the variable P_{gly} appearing in the function f_1, represents the influence of the glycerol permeability on the critical relevance of gluconeogenesis in determining the hepatic glucose dynamics. In the proposed model the regulatory mechanism of hepatic AQP9 protein output as function of h(I) and the P_{gly} value as function of the hepatic AQP9 protein are described for the first time. The mathematical expression of h(I) and $P_{gly}(A)$ have been experimentally derived using nonlinear fitting based on Hill function as described in the *Results* section. Hill functions are largely used to describe the pattern of curve shapes for most biochemical reactions and, more in general, biological input-output relationships (Alon, 2006; DiStefano, 2015). Hill function of order 2 could be used, for instance, to represent a positively regulated glucose-dependent nonlinear source term in the function f_2.

2.9. Statistical analysis

Experiments with each group of animals were performed at least in triplicate. All data resulting from three to five independent preparations were expressed as mean ± S.E.M. Data were analyzed statistically by the Student's *t*-test. Results were considered statistically significant when $P < 0.05$.

3. Results

To set up a mathematical model capable to simulate the changes in male murine hepatic glycerol permeability (P_{gly}) in function of the different nutritional states we started by assessing experimentally the time course of the major metabolic parameters modulating hepatic AQP9 expression and P_{gly}.

3.1. Analysis of plasma glucose, insulin and glycerol and hepatic glycogen stores

Mice were kept in the fed, fasted (48 h) or re-fed states (72 h) and the (*i*) plasma levels of glucose, glycerol and insulin and the hepatic (*ii*) expression of AQP9 protein, and (*iii*) extent of glycogen stores were measured at defined time intervals as described in *Materials and Methods*. The impact of fasting and re-feeding conditions was also checked by measuring the mean body weight of the animals at these two different nutritional states compared to the mean body weight value assessed at the fed state, before the fast-

Table 1
Mean body weight of mice at the fed, fasted and re-fed states.

	Fed	Fasted (48 h)	Re-fed (72 h)
Body weight (grams)	22.83 ± 0.36 (n = 22)	16.94 ± 0.57** (n = 22)	22.95 ± 0.29 (n = 22)

** P < 0.0001.

ing period (Table 1). Samples of each mouse liver specimen were used to evaluate the hepatic glycerol permeability (see below) after preparing vesicles of the sinusoidal plasma membrane of hepatocytes. As expected, starvation led to a significant reduction of the body weight and plasma glucose whose levels, after re-feeding, returned to the ones measured at the initial fed state (Table 1 and Fig. 1**A**). In terms of circulating insulin, the decrease induced by fasting was reversed when the animals were re-fed (Fig. 1**B**). In line with our previous work (Calamita et al., 2012) and consistent with the significance of lipolytic glycerol as main source of gluconeogenesis in short-term fasting, 24–30 h of starvation led to a significant increase of plasma glycerol whose levels returned to the basal extent after 60 h of re-feeding (Fig. 1**C**).

Hepatic glucose output results from the contribution of *de novo* synthesis *via* gluconeogenesis and/or from degradation of hepatic glycogen *via* glycogenolysis. Hence, samples of each mouse liver specimen were used to assess the time course of hepatic glycogen storage in the various experimental conditions. Glycogen stores were assayed biochemically after alkaline extraction as described in *Materials and Methods*. As expected, short term fasting was accompanied by a marked increase in the rate of glycogenolysis leading to a strong reduction of the glycogen stores. Glycogen started to be re-accumulated within liver parenchyma when mice regained access to food (Fig. 2). These changes in hepatic glycogen content were fully confirmed by the histochemical analysis carried out with sections of the same liver samples (Fig. 3**A**–**F**).

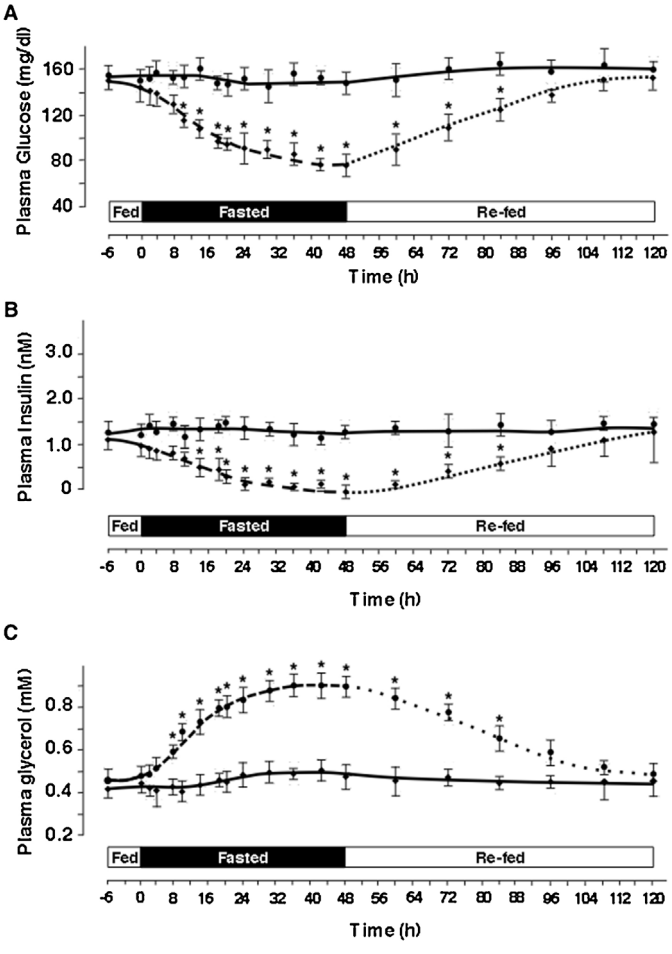

Fig. 1. Effect of feeding, fasting and re-feeding on the plasma levels of glucose, insulin and glycerol. Plasma was prepared from blood samples collected from male mice sacrificed at various time points in fed state (*full line*), fasted (*dashed line*) or re-fed (*dotted line*) conditions. Values are compared to those of mice always kept in fed state (*continuous full line*). Plasma glucose (**A**), insulin (**B**) and glycerol (**C**) were assayed as described in *Materials and Methods*. Data are mean ± S.E.M. from 4 to 5 independent plasma samples. Asterisk (*), $P < 0.01$ (fed, fasted or re-fed state *vs.* corresponding time point of mice constantly kept in fed state).

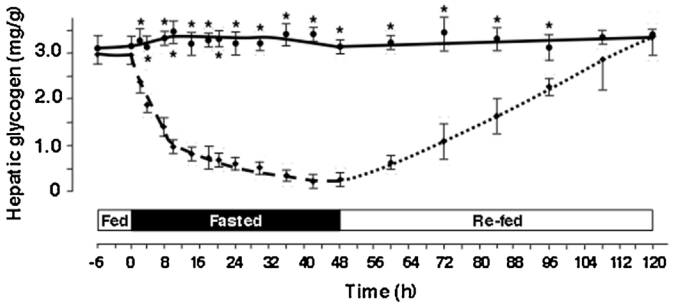

Fig. 2. Changes of glycogen stores. Male mice were sacrificed in fed state or after 0, 2, 4, 8, 14, 18, 20, 24, 30, 36, and 48 h of fasting or 12, 24, 36, 48, 60 and 72 h of re-feeding following the fasting and then livers removed for analyses. Glycogen content in mouse liver parenchyma (milligrams per gram of hepatic mass) is from fed (*full line*), 48 h-fasted (*dashed line*) or after 72 h-re-feeding (*dotted line*). Values are compared to those of mice constantly kept in fed state (*continuous full line*). Glycogen storage was determined spectrophotometrically as described in *Materials and Methods*. The values are presented as mean ± S.E.M. of 4–5 mice per group. Asterisk (*), $P < 0.01$ (fed, fasted or re-fed state *vs.* corresponding time point of mice constantly kept in fed state).

3.2. Hepatic AQP9 and glycerol permeability during short term fasting and re-feeding

In a next step, the levels of hepatic AQP9 protein were analyzed in the different nutritional states. The extent of AQP9 protein was measured by semi-quantitative immunoblotting using a gravitational membrane fraction enriched in hepatocyte sinusoidal plasma membranes (see *Materials and methods*). Consistent with a previous work (Calamita et al., 2012), immunoreactive bands of 32 and 37–43 kDa were detected corresponding to the core and N-glycosylated (glycoAQP9) forms of the AQP9 protein, respectively. In line with the above results and role of AQP9 as glycerol channel, the levels of AQP9 were significantly higher in the fasted state (18–20 h of starvation) than the fed or fasted/re-fed states (Fig. 4**A**). Fig. 4**B** reports the time course of AQP9 expression in the liver of the fed, fasted or re-fed mice. Hepatic AQP9 increased in the first 18–24 h of fasting while decreased considerably in the following 16–24 h of starvation. Seventy-hours of re-feeding returned AQP9 to the levels measured at the fed state (Fig. 4**B**).

Hepatic glycerol permeability (P_{gly}, 10^{-6} cm/s) was assessed by stopped-flow light scattering using aliquots of the hepatocyte sinusoidal membranes vesicle specimens employed to determine the AQP9 protein in the different nutritional conditions. To measure the hepatic glycerol permeability, membrane vesicles were submitted to a 150 mM inwardly directed gradient of glycerol, as described in *Materials and Methods*. In line with our previous study, hepatic P_{gly} changed accordingly with the AQP9 protein values. Glycerol

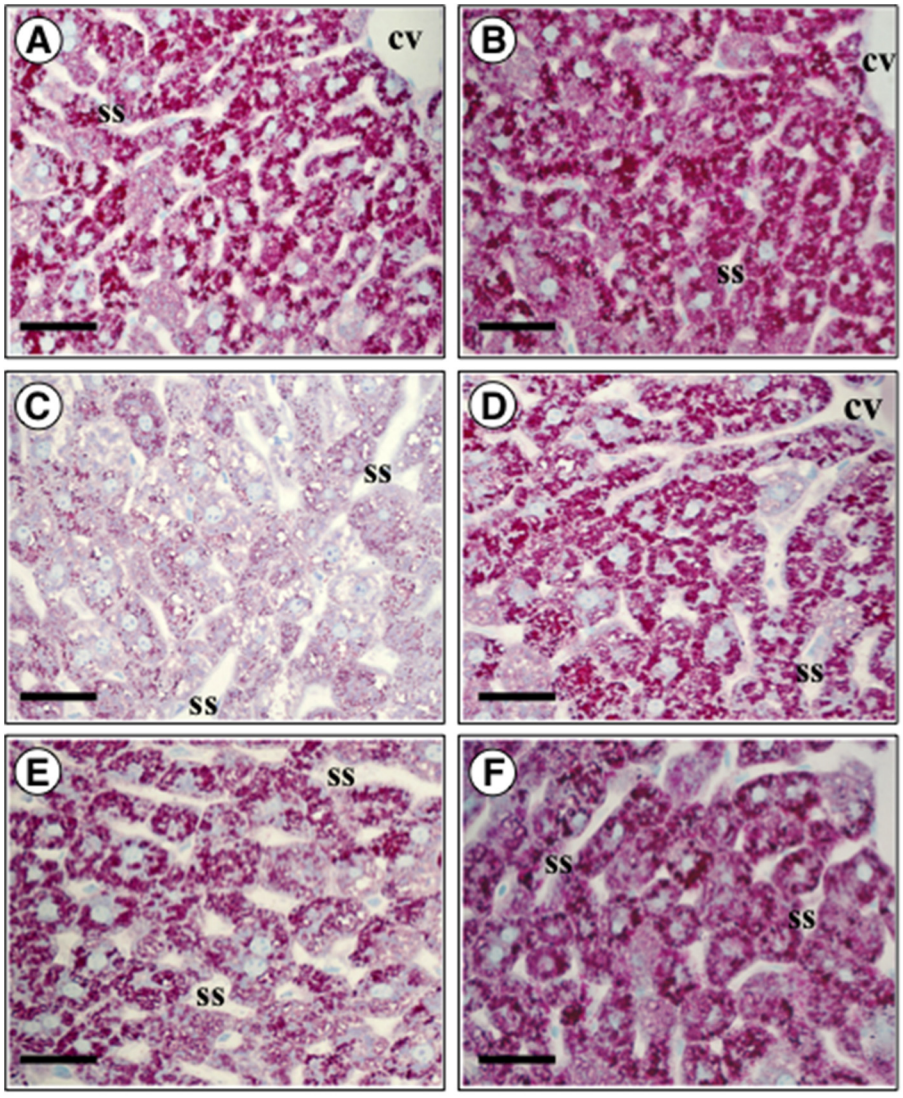

Fig. 3. Histochemical analysis of hepatic glycogen stores. Liver sections were stained with toluidine blue (TB)-periodic acid-Schiff (PAS) as described in *Materials and Methods*. **A**, **C** and **E**, sections from fed (**B**), fasted (48 h; **D**) and re-fed (72 h of re-feeding after 48 h of fasting; **F**) mice, respectively. **B**, **D** and **F**, liver sections from mice kept in the fed state at time points 0-h, 48-h and 120-h (as from Fig. 2), respectively. Red staining indicates glycogen stores. **cv**, centrolobular vein; **ss**, sinusoidal space; *bar*, 25 μm. (For interpretation of the references to colour in this figure legend, the reader is referred to the web version of this article.)

permeability steadily increased during fasting reaching the highest levels in the first 16–24 h and declining in the following 30 h of starvation (Fig. 5). Hepatic P_{gly} returned to the basal values after 30–36 h of re-feeding (Fig. 5).

3.3. Approximation of liver glycerol import through AQP9 in the fasting state

To set up a mathematical expression of the functions h(I) and P_{gly} (A) correlating the protein levels of AQP9 and expected value of insulin and glycerol permeability, respectively, we focused on the AQP9-mediated permeation of glycerol within liver parenchyma. The liver glycerol permeability was assumed to depend only on the level *A* of the AQP9 protein during the fasting state, when hepatocyte AQP9 is of maximal importance in mediating the import of glycerol from the sinusoidal blood (Calamita et al., 2012).

The experimental observations were collected in a dataset containing 20 pairs of P_{gly} and sinusoidal AQP9 protein values. The dependence of P_{gly} from *A* was approximated using least squares regression models. Data fitting in the least squares sense is a model approximation approach particularly useful when curvilinear effects are present in the true response function or when very complex nonlinear relationships are supposed to exist between experimental data.

We approximated the experimental data using a nonlinear least squares model based on Hill function of the form

$$\text{Hill}(x) = \beta_1 + (\beta_2 - \beta_1)/(1 + \theta^n/x^n)$$

where β_i (i = 1,2) and θ are real parameters and *n* is the degree of Hill function assumed to be integer. Particularly, positive values of the degree *n* provide an ascending curve while negative values model a descending behavior (Alon, 2006; Gadagkar and Call, 2015).

The parameter values were obtained using the least squares method, while the degree *n* of the Hill model which "best" fits the data was estimated by the 10-fold Cross Validation method (to reduce variability, multiple rounds of 10 cross-validation are performed using different partitions, and the validation results were averaged over the rounds). Accordingly to the obtained results, the smallest mean value error was obtained using the following third degree Hill function:

$$P_{gly}(A) = 8.6741 + (16.2616 - 8.6741)/(1 + 2.1464^3/A^3) \quad (1)$$

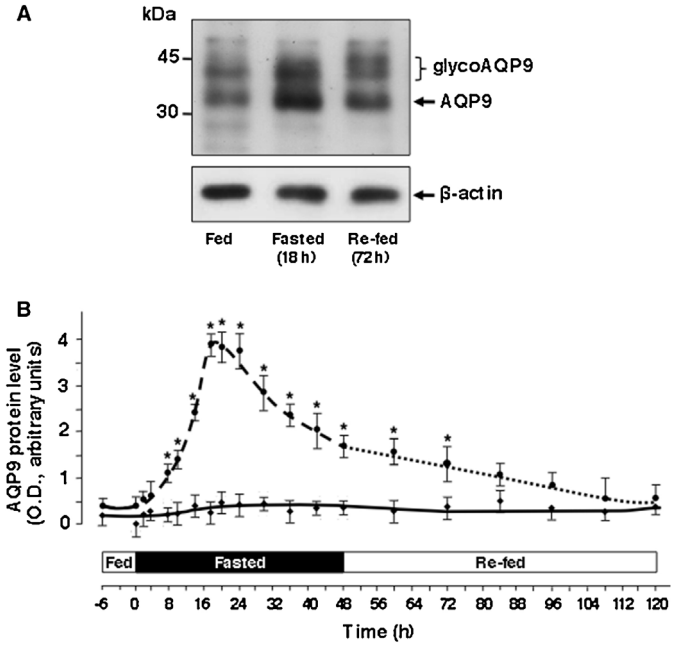

Fig. 4. Hepatic expression of AQP9 in various nutritional conditions. **A**, representative immunoblot using an anti-AQP9 antibody showing the distribution of AQP9 among hepatocyte sinusoidal membrane fractions prepared from liver homogenates of fed, fasted (18 h) and re-fed (72 h) mice. AQP9 is detected as immunoreactive bands of 32 and 37–43 kDa, corresponding to the core (AQP9) and glycosylated (glycoAQP9) forms of the protein, respectively. The lower panel shows the expression of ß-actin, a housekeeping protein used to normalize the expression of AQP9. **B**, time course of AQP9 protein levels, expressed as the optic density (O.D.) of AQP9 and glycoAQP9 immunoreactive bands, in hepatocyte sinusoidal plasma membrane of livers from mice in fed (*full line*), fasted (*dashed line*) or re-fed (*dotted line*) state expressed as optic density of AQP9 and glycoAQP9 immunoreactive bands. The values are presented as mean ± S.E.M. of 4–5 mice per group. Asterisk (*), $P < 0.01$ (fed, fasted or re-fed state *vs.* corresponding time point of mice constantly kept in fed state).

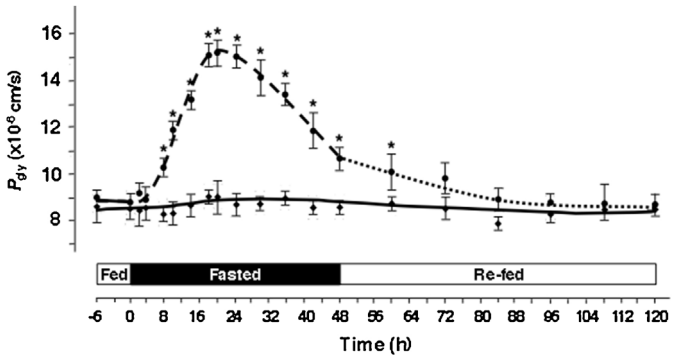

Fig. 5. Time course of changes of the coefficient of glycerol permeability (P_{gly}) of hepatocyte sinusoidal membrane of male mice at various time points of fed (*full line*), fasted (*dashed line*) or re-fed (*dotted line*) state. Glycerol permeability was measured by stopped-flow light scattering as described in *Materials and Methods*. Paralleling the expression of hepatic AQP9, the highest values of P_{gly} were measured after 18–24 h of fasting. Asterisk (*), $P < 0.01$ (fasted or re-fed state *vs.* corresponding time point of fed state).

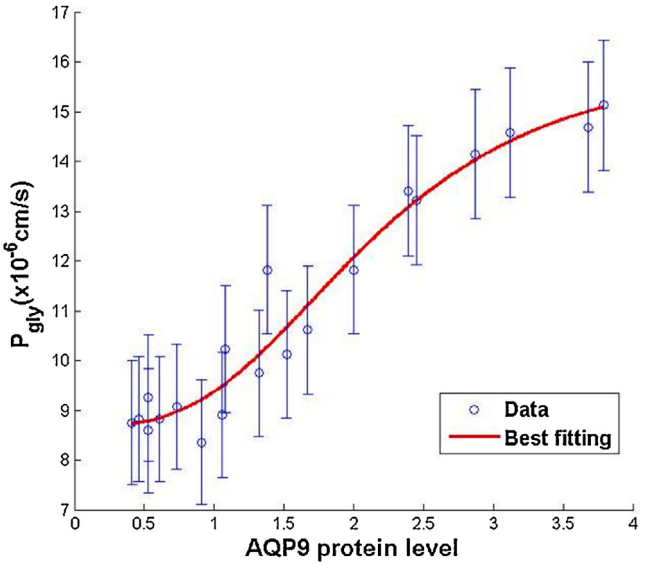

Fig. 6. Graphical illustration of the third degree increasing Hill function fitting P_{gly} as function of AQP9. The *continuous red line* represents the graph of the mathematical function reported in Eq. (1) for the AQP9 protein levels, expressed as the optic density (O.D.) of AQP9 and glycoAQP9 immunoreactive bands, in the interval [0,4]. *Blue circles* represent the experimental data whereas *blue error bar* indicate the errors between experimental observations and predicted mathematical value. (For interpretation of the references to colour in this figure legend, the reader is referred to the web version of this article.)

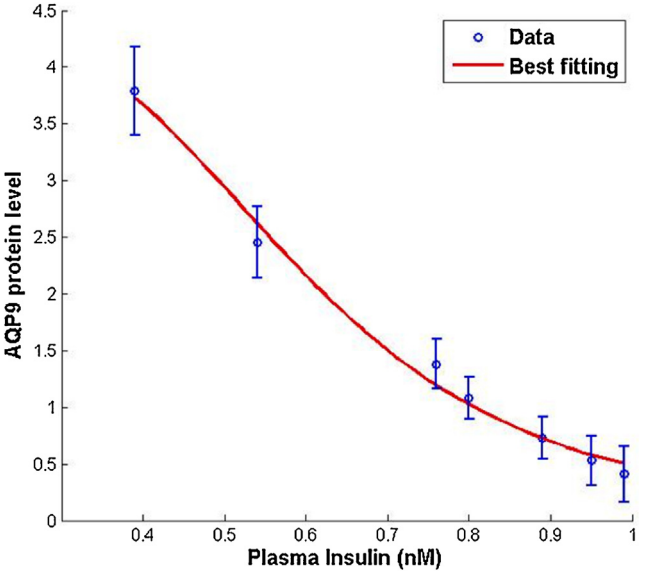

Fig. 7. Graphical illustration of the fourth degree decreasing Hill function best fitting the experimental values of circulating insulin. The *continuous red line* represents the graph of the obtained Hill function in the range interval of given data whereas *blue circles* represent the experimental data coming from the immunoblotting analysis (levels of AQP9 protein) and plasma biochemistry (circulating insulin). (For interpretation of the references to colour in this figure legend, the reader is referred to the web version of this article.)

The behavior of the best fitting 3° Hill function in (1) against the given data (depicted as blue circles) and the error bar corresponding to each data point is illustrated in Fig. 6.

Hill based nonlinear regression model with descending behavior (*i.e.*, with negative degree value n) was adopted to best fit the experimental data composed of 7 observation values of circulating insulin and AQP9 protein. However, in this case, due to the reduced number of examples, a single trial was performed. The smallest mean value error (in least squared sense) was obtained using the fourth degree descending ($n = -4$) Hill function

$$h(I) = 0.0030 + (4.4255–0.0030)/(1 + I^4/0.5928^4)$$

Fig. 7 shows the best fitting Hill function (depicted as a continuous red curve) against the given data (depicted as blue circles) and

the error bar corresponding to each data point. Finally, the system of ODEs becomes:

$$dG/dt = f_1(G, I, \Gamma, P_{gly}(A))$$

$$dI/dt = f_2(G, I)$$

$$d\Gamma/dt = f_3(G, \Gamma)$$

$$dA/dt = 0.0030 + (4.4255–0.0030)/(1 + I^4/0.5928^4) - \alpha A$$

where the function $P_{gly}(A)$ is described in Eq. (1).

We finally observed that the results obtained with least squares fitting models would not be reliable for values of the predictor variables outside the range of the experimental data.

4. Discussion

Liver is the main organ controlling energy metabolism and hepatocytes exhibit high capacity of glycogenesis, glycogenolysis, glycolysis and gluconeogenesis enabling them to temporarily store considerable amounts of glucose as glycogen, to newly synthesized glucose from different sources. In its phosphorylated form (G3P), glycerol is an important gluconeogenetic substrate, especially during short term fasting. Glycerol utilization by hepatocytes is rate-limited by the permeation step through the sinusoidal plasma membrane (Li and Lin, 1983) and AQP9 has been proved to be the major pathway through which glucogenetic glycerol is imported from the portal blood, especially during short-term fasting (Calamita et al., 2012; Jelen et al., 2011). As a matter of fact, *Aqp9* knockout mice did not show any increase in hepatic P_{gly} during short-term fasting whereas no other known mouse glycerol facilitators, namely AQP3 and AQP7 (*Aqp10* is a pseudogene in mouse), appeared to be detected in the liver parenchyma of the same animals. This was consistent with the observation that the hepatic glycerol permeability of the AQP9-ablated mice does not diminish after treatment with phloretin, a blocker of the facilitated glycerol transport (Calamita et al., 2012). A recent work by Gregoire et al. reported transcriptional expression of *Aqp3* and *Aqp7* (in addition to *Aqp9*) in primary murine hepatocytes (Gregoire et al., 2015). This suggests that the expression profile of hepatocyte aquaglyceroporins may change *in vitro* conditions.

A series of detailed kinetic models of human glucose metabolism concentrating on inter-convertible metabolic enzymes and/or insulin and its antagonists glucagon and epinephrine are already available (Bulik et al., 2016; Chalhoub et al., 2007; König et al., 2012; Silber et al., 2010). However, a mathematical model of hepatic glucose metabolism integrating the hepatic uptake of glucoplastic glycerol and the dynamical role played by AQP9 in this process is lacking, so far. Recently, we approached the question by describing a model of human hepatic glucose metabolism based on Hill and step functions (D'Abbicco et al., 2016). As initial step, we decided to model critical parameters such as the changes of glycogen stores associated to the fed and fasted states and the influence of plasma glycerol and hepatic glycerol permeability in glucose homeostasis. As a next step, in the present work, we added two novel and critical hepatic variables such as the output of liver AQP9 protein and the hepatic permeability to glycerol. Based on the experimental data obtained using male murine models we derive, for the first time, a correlation between the two variables. We also tentatively describe the expression of AQP9 at the sinusoidal plasma membrane by means of a first-order ordinary differential equation where we assumed the linear degradation rate with a half-life time of 8 h, and derived a production rate function, the latter known to be down-regulated by circulating insulin. Limitations of our model cannot be completely ruled out since hepatocyte AQP9 protein might be also controlled by agents other than insulin acting on the degradation of the protein. The signaling pathway and related control underlying liver AQP9 degradation will be matter of further studies. The linear function used in the proposed model is therefore the simplest option in modeling the degradation of the protein. After all, the acquired data do not permit to completely parameterize the whole model.

The liver glycerol permeability (Pgly) as a function of the hepatocyte AQP9 expression is assumed to appear as a source term in the ordinary differential equation that regulates the variable G representing the hepatic glucose. Due to the large number of mechanisms and variables involved, no speculation appears to be possible in absence of a huge amount of experimental data for the measurements of glycerol permeability levels in different time points of the fasting state for a large population of subjects. The only educated guess which may be formulated is that a very simple model for function f_1 should include: a linear component (of the form $-c_1G$) representing the insulin independent glucose utilization, a nonlinear term ($-c_2IG$) representing the insulin dependent glucose utilization, and some source terms related to glycogenolysis and glycerol membrane permeability which are negatively regulated by insulin values. Still, derived abstract model can be used to tentatively describe from a mathematical point of view the dynamics of the AQP9 involvement in hepatic glucose metabolism providing useful predictive information on how the liver glycerol permeability changes as a direct function of the AQP9 protein at the sinusoidal plasma membrane of hepatocyte. The correlation between circulating insulin and hepatocyte AQP9 is also derived constituting, to our knowledge, a novelty in the field of aquaporin channels. The obtained abstract model is a tool to underlie the critical importance of modulating the levels of AQP9 and the extent of glycerol permeability to adapt the hepatic metabolism to the different nutritional states acting on plasma glucose levels, hormonal signals and content of glycogen stores within liver parenchyma. The obtained data are also important for the fully understanding of the role of the liver in glucose homeostasis, which is not always completely accessible experimentally.

Consistent with previous studies, the highest extent of mouse liver glycerol permeability is measured after 18–24 h of starvation (Calamita et al., 2012), when glycerol constitutes the main substrate sustaining hepatic gluconeogenesis (Landau et al., 1996; Peroni et al., 1996), before declining gradually in the following 16–30 h of fasting, when the glucoplastic action of this metabolic intermediate is steadily replaced by other sources in supplying the hepatocyte glucose output (Reshef et al., 2003). This profile fits well with the changes of the expression levels of AQP9 in the liver of mice in different nutritional conditions. Moreover, the hepatic P_{gly} and AQP9 protein are both inversely correlated with the liver glycogen whose stores are almost completely emptied after 10–15 h of fasting. While the main function of hepatocyte AQP9 seems to be that of importing glycerol in short term fasting this aquaporin might be of pleiotropic relevance to liver physiology as, in fed conditions, it has been suggested to contribute to the extrusion of catabolic urea (Jelen et al., 2012) and the import of water in primary bile formation (Calamita et al., 2008).

Mathematical models are often an abstraction of reality describing multiple aspects of biological phenomena. Even so, it is necessary to make some assumptions to figure out both the range of model application and the limitations. The results of this work refer to the normal physiological situation of male lean C57BL/6J mice fed a standard diet where significant changes of the blood glucose level occur in a time lapse of hours (Figs. 1–5) with the metabolic network always being in quasi-steady state. The model is also limited to physiological states of the liver where changes in the energy and redox state can be neglected. Since the hepatic energy condition is normally decoupled from the hepatocyte glu-

cose metabolism, with β-oxidation of fatty acids providing ATP and reduced redox equivalents (NADH), our model is not able to simulate situations such as those created under hypoxic or ischemic conditions. A further limitation is that of describing the metabolic net behavior of the liver of a hepatocyte averaged over the whole liver parenchyma. The model is therefore able only to simulate the net effect of the liver on glucose balance. Considerable differences exist in the coordinated regulation of fat-specific AQP7 and liver-specific AQP9 in determining glucose metabolism between healthy and insulin resistant rodents (Calamita et al., 2015; Hirako et al., 2015; Lebeck, 2014). Hence, mathematical modeling of glycerol permeability and aquaglyceroporins expression should take into account the peculiarities of the specific patho-physiological condition especially when applying to metabolic disorders with altered glucose metabolism.

Hepatic handling of glycerol is not fully comparable between humans and rodents (Reshef et al., 2003). In line with this, the hepatic metabolism of the AQP9-imported glycerol is reported to be quite distinct between man and rat or mouse (for review see Rodriguez et al., 2015a). However, both in humans and rodents, both the expression and hormonal control of liver AQP9 undergo gender dimorphism (for review see Rodriguez et al., 2015a). In humans, the higher expression of hepatocyte AQP9 in males than females seems to reflect the known preference of carbohydrate metabolism in men and lipid in women. These distinctions should not be disregarded in future mathematical models involving human hepatic AQP9 and glycerol permeability.

In conclusion, our mathematical model may represent a valuable tool in understanding the mechanistic relationships involving AQP9 and glycerol in rodent liver glucose metabolism. Moreover, the model has good premises to be adapted and integrated to models of human whole-body glucose metabolism, especially in reproducing the dynamics of glucose and energy homeostasis in health and diseases accompanied by metabolic disorders.

Acknowledgments

Financial support from “Fondazione Cassa di Risparmio di Puglia” (Viale della Repubblica 111, 70125 Bari, Italy) through the project “Modelli Matematici Discontinui per l'Analisi delle Reti di Geni: Applicazioni al Diabete” (2012–2013) and from Regione Puglia (Rete di Laboratori Pubblici di Ricerca WAFITECH-cod. 09) is gratefully acknowledged.

References

Agre, P., 2004. Nobel lecture. Aquaporin water channels. Angew. Chem. Int. Ed. Engl. 43, 4278–4290.
Alon, U., 2006. An introduction to systems biology: design principles of biological circuits. In: Chapman, Hall (Eds.), Mathematical and Computational Biology Series. CRC Press Taylor and Francis Group, Boca Raton, Fl.
Badaut, J., Petit, J.M., Brunet, J.F., Magistretti, P.J., Charriaut-Marlangue, C., Regli, L., 2004. Distribution of Aquaporin 9 in the adult rat brain: preferential expression in catecholaminergic neurons and in glial cells. Neuroscience 128, 27–38.
Bernardino, R.L., Marinelli, R.A., Maggio, A., Gena, P., Cataldo, I., Alves, M.G., Svelto, M., Oliveira, P.F., Calamita, G., 2016. Hepatocyte and Sertoli cell aquaporins, recent advances and research trends. Int. J. Mol. Sci. 17, 1096.
Brisson, D., Vohl, M.C., St-Pierre, J., Hudson, T.J., Gaudet, D., 2001. Glycerol: a neglected variable in metabolic processes? Bioessays 23, 534–542.
Bulik, S., Holzhütter, H.G., Berndt, N., 2016. The relative importance of kinetic mechanisms and variable enzyme abundances for the regulation of hepatic glucose metabolism–insights from mathematical modeling. BMC Biol. 14, 15.
Calamita, G., Ferri, D., Gena, P., Carreras, F.I., Liquori, G.E., Portincasa, P., Marinelli, R.A., Svelto, M., 2008. Altered expression and distribution of aquaporin-9 in the liver of rat with obstructive extrahepatic cholestasis. Am. J. Physiol. Gastrointest. Liver Physiol. 295, G682–690.
Calamita, G., Gena, P., Ferri, D., Rosito, A., Rojek, A., Nielsen, S., Marinelli, R.A., Fruhbeck, G., Svelto, M., 2012. Biophysical assessment of aquaporin-9 as principal facilitative pathway in mouse liver import of glucogenetic glycerol. Biol. Cell 104, 342–351.
Calamita, G., Delporte, C., Marinelli, R.A., 2015. Hepatobiliary, salivary glands and pancreas aquaporins in health and disease. In: Soveral, G., Nielsen, S., Casini, A. (Eds.), Aquaporins in Health and Disease: New Molecular Targets for Drug Discovery. CRC Press Taylor & Francis Group, Boca Raton, Fl, pp. 193–196, Chapter 9.
Carbrey, J.M., Gorelick-Feldman, D.A., Kozono, D., Praetorius, J., Nielsen, S., Agre, P., 2003. Aquaglyceroporin AQP9: solute permeation and metabolic control of expression in liver. Proc. Natl. Acad. Sci. U. S. A. 100, 2945–2950.
Chalhoub, E., Xie, L., Balasubramanian, V., Kim, J., Belovich, J., 2007. A distributed model of carbohydrate transport and metabolism in the liver during rest and high-intensity exercise. Ann. Biomed. Eng. 35, 474–491.
Chen, C.L., Tsai, H.W., Wong, S.S., 2010. Modeling the physiological glucose-insulin dynamic system on diabetics. J. Theor. Biol. 265, 314–322.
D'Abbicco, M., Del Buono, N., Gena, P., Berardi, M., Calamita, G., Lopez, L., 2016. A model for the hepatic glucose metabolism based on Hill and step functions. J. Comput. Appl. Math. 292, 746–759.
Del Buono, N., Elia, C., Lopez, L., 2014. On the equivalence between the sigmoidal approach and Utkin's approach for piecewise-linear models of gene regulatory networks. SIAM J. Appl. Dyn. Syst. 13, 1270–1292.
DiStefano, J., 2015. Dynamic Systems Biology Modeling and Simulation, first edition. Academic Press, London.
Elkjaer, M., Vajda, Z., Nejsum, L.N., Kwon, T., Jensen, U.B., Amiry-Moghaddam, M., Frokiaer, J., Nielsen, S., 2000. Immunolocalization of AQP9 in liver, epididymis, testis, spleen, and brain. Biochem. Biophys. Res. Commun. 276, 1118–1128.
Ferri, D., Mazzone, A., Liquori, G.E., Cassano, G., Svelto, M., Calamita, G., 2003. Ontogeny, distribution, and possible functional implications of an unusual aquaporin, AQP8, in mouse liver. Hepatology 38, 947–957.
Gadagkar, S.G., Call, G.B., 2015. Computational tools for fitting the Hill equation to dose–response curves. J. Pharmacol. Toxicol. Methods 71, 68–76.
Gena, P., Pellegrini-Calace, M., Biasco, A., Svelto, M., Calamita, G., 2011. Aquaporin membrane channels: biophysics, classification, functions, and possible biotechnological applications. Food Biophys. 6, 241–249.
Gena, P., Mastrodonato, M., Portincasa, P., Fanelli, E., Mentino, D., Rodriguez, A., Marinelli, R.A., Brenner, C., Fruhbeck, G., Svelto, M., Calamita, G., 2013. Liver glycerol permeability and aquaporin-9 are dysregulated in a murine model of non-alcoholic fatty liver disease. PLoS One 8, e78139.
Gregoire, F., Lucidi, V., Zerrad-Saadi, A., Virreira, M., Bolaky, N., Delforge, V., Lemmers, A., Donckier, V., Devière, J., Demetter, P., Perret, J., Delporte, C., 2015. Analysis of aquaporin expression in liver with a focus on hepatocytes. Histochem. Cell Biol. 144, 347–363.
Hara-Chikuma, M., Verkman, A.S., 2006. Physiological roles of glycerol-transporting aquaporins: the aquaglyceroporins. Cell. Mol. Life Sci. 63, 1386–1392.
Hirako, S., Wakayama, Y., Ki, m.H., Iizuka, Y., Matsumoto, A., Wada, N., Kimura, A., Okabe, M., Sakagami, J., Suzuki, M., Takenoya, F., Shioda, S., 2015. The relationship between aquaglyceroporin expression and development of fatty liver in diet-induced obesity and ob/ob mice. Obes. Res. Clin. Pract. S1871-403X (15), 00200–00208.
Ishibashi, K., Kuwahara, M., Gu, Y., Tanaka, Y., Marumo, F., Sasaki, S., 1998. Cloning and functional expression of a new aquaporin (AQP9) abundantly expressed in the peripheral leukocytes permeable to water and urea, but not to glycerol. Biochem. Biophys. Res. Commun. 244, 268–274.
Jelen, S., Wacker, S., Aponte-Santamaria, C., Skott, M., Rojek, A., Johanson, U., Kjellbom, P., Nielsen, S., de Groot, B.L., Rutzler, M., 2011. Aquaporin-9 protein is the primary route of hepatocyte glycerol uptake for glycerol gluconeogenesis in mice. J. Biol. Chem. 286, 44319–44325.
Jelen, S., Gena, P., Lebeck, J., Rojek, A., Praetorius, J., Frøkiaer, J., Fenton, R.A., Nielsen, S., Calamita, G., Rützler, M., 2012. Aquaporin-9 and urea transporter-A gene deletions affect urea transmembrane passage in murine hepatocytes. Am. J. Physiol. Gastrointest. Liver Physiol. 303, G1279–G1287.
König, M., Bulik, S., Holzhutter, H.G., 2012. Quantifying the contribution of the liver to glucose homeostasis: a detailed kinetic model of human hepatic glucose metabolism. PLoS Comput. Biol. 8, e1002577.
Kuriyama, H., Shimomura, I., Kishida, K., Kondo, H., Furuyama, N., Nishizawa, H., Maeda, N., Matsuda, M., Nagaretani, H., Kihara, S., Nakamura, T., Tochino, Y., Funahashi, T., Matsuzawa, Y., 2002. Coordinated regulation of fat-specific and liver-specific glycerol channels, aquaporin adipose and aquaporin 9. Diabetes 51, 2915–2921.
Landau, B.R., Wahren, J., Chandramouli, V., Schumann, W.C., Ekberg, K., Kalhan, S.C., 1996. Contributions of gluconeogenesis to glucose production in the fasted state. J. Clin. Invest. 98, 378–385.
Lebeck, J., 2014. Metabolic impact of the glycerol channels AQP7 e AQP9 in adipose tisue and liver. J. Mol. Endocrinol. 52, R165–178.
Li, C.C., Lin, E.C., 1983. Glycerol transport and phosphorylation by rat hepatocytes. J. Cell. Physiol. 117, 230–234.
Lindskog, C., Asplund, A., Catrina, A., Nielsen, S., Rützler, M., 2016. A systematic characterization of aquaporin-9 expression in human normal and pathological tissues. J. Histochem. Cytochem. 64, 287–300.
Liu, Z., Shen, J., Carbrey, J.M., Mukhopadhyay, R., Agre, P., Rosen, B.P., 2002. Arsenite transport by mammalian aquaglyceroporins AQP7 and AQP9. Proc. Natl. Acad. Sci. U. S. A. 99, 6053–6058.
Marinelli, R.A., Tietz, P.S., Caride, A.J., Huang, B.Q., LaRusso, N.F., 2003. Water transporting properties of hepatocyte basolateral and canalicular plasma membrane domains. J. Biol. Chem. 278, 43157–43162.
Palumbo, P., Ditlevsen, S., Bertuzzi, A., De Gaetano, A., 2013. Mathematical modeling of the glucose-insulin system: a review. Math. Biosci. 244, 69–81.
Pastor-Soler, N., Bagnis, C., Sabolic, I., Tyszkowski, R., McKee, M., Van Hoek, A., Breton, S., Brown, D., 2001. Aquaporin 9 expression along the male reproductive tract. Biol. Reprod. 65, 384–393.

Peroni, O., Large, V., Odeon, M., Beylot, M., 1996. Measuring glycerol turnover, gluconeogenesis from glycerol, and total gluconeogenesis with [2-^{13}C] glycerol: role of the infusion-sampling mode. Metabolism 45, 897–901.

Reshef, L., Olswang, Y., Cassuto, H., Blum, B., Croniger, C.M., Kalhan, S.C., Tilghman, S.M., Hanson, R.W., 2003. Glyceroneogenesis and the triglyceride/fatty acid cycle. J. Biol. Chem. 278, 30413–30416.

Rodríguez, A., Catalán, V., Gómez-Ambrosi, J., Frühbeck, G., 2011a. Aquaglyceroporins serve as metabolic gateways in adiposity and insulin resistance control. ABBV Cell Cycle 10, 1548–1556.

Rodríguez, A., Catálan, V., Gómez-Ambrosi, J., García-Navarro, S., Rotellar, F., Valentí, V., Silva, C., Gil, M.J., Salvador, J., Calamita, G., Malagón, M.M., Frühbeck, G., 2011b. Insulin- and leptin-mediated control of aquaglyceroporins in human adipocytes and hepatocytes is mediated via the PI3K/Akt/mTOR signaling cascade. J. Clin. Endocrinol. Metab. 96, 586–597.

Rodriguez, A., Gena, P., Mendez-Gimenez, L., Rosito, A., Valenti, V., Rotellar, F., Sola, I., Moncada, R., Silva, C., Svelto, M., Salvador, J., Calamita, G., Frühbeck, G., 2014. Reduced hepatic aquaporin-9 and glycerol permeability are related to insulin resistance in non-alcoholic fatty liver disease. Int J. Obes. (Lond.) 38, 1213–1220.

Rodríguez, A., Marinelli, R.A., Tesse, A., Frühbeck, G., Calamita, G., 2015a. Sexual dimorphism of adipose and hepatic aquaglyceroporins in health and metabolic disorders. Front. Endocrinol. (Lausanne) 6, 171.

Rodríguez, A., Moreno, N.R., Balaguer, I., Méndez-Giménez, L., Becerril, S., Catalán, V., Gómez-Ambrosi, J., Portincasa, P., Calamita, G., Soveral, G., Malagón, M.M., Frühbeck, G., 2015b. Leptin administration restores the altered adipose and hepatic expression of aquaglyceroporins improving the non-alcoholic fatty liver of ob/ob mice. Sci. Rep. 5, 12067.

Rojek, A.M., Skowronski, M.T., Fuchtbauer, E.M., Fuchtbauer, A.C., Fenton, R.A., Agre, P., Frokiaer, J., Nielsen, S., 2007. Defective glycerol metabolism in aquaporin 9 (AQP9) knockout mice. Proc. Natl. Acad. Sci. U. S. A. 104, 3609–3614.

Silber, H.E., Jauslin, P.M., Frey, N., Karlsson, M.O., 2010. An integrated model for the glucose-insulin system. Basic Clin. Pharmacol. Toxicol. 106, 189–194.

Sprangers, F., Sauerwein, H.P., Romijn, J.A., van Woerkom, G.M., Meijer, A.J., 1998. Nitric oxide inhibits glycogen synthesis in isolated rat hepatocytes. Biochem. J. 330, 1045–1049.

Tsukaguchi, H., Shayakul, C., Berger, U.V., Mackenzie, B., Devidas, S., Guggino, W.B., van Hoek, A.N., Hediger, M.A., 1998. Molecular characterization of a broad selectivity neutral solute channel. J. Biol. Chem. 273, 24737–24743.